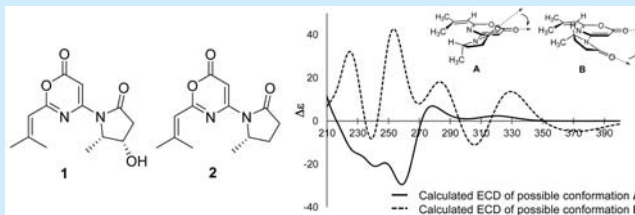


Salinazinones A and B: Pyrrolidinyl-Oxazinones from Solar Saltern-Derived *Streptomyces* sp. KMF-004Min Cheol Kim,^{†,#} Jung Hwan Lee,^{†,‡,#} Bora Shin,[§] Lalita Subedi,^{||,⊥} Jin Wook Cha,[†] Jin-Soo Park,[†] Dong-Chan Oh,[§] Sun Yeou Kim,^{||,⊥} and Hak Cheol Kwon^{*,†}[†]Natural Products Research Center, Korea Institute of Science and Technology (KIST), Gangneung, Gangwon-do 210-340, Republic of Korea[‡]Department of Marine Molecular Biotechnology, Gangneung-Wonju National University, Gangwon-do 210-702, Republic of Korea[§]Natural Products Research Institute, College of Pharmacy, Seoul National University, Seoul 151-742, Republic of Korea^{||}College of Pharmacy, Gachon University, Yeonsu-gu, Incheon 40-799, Republic of Korea[⊥]Gachon Institute of Pharmaceutical Science, Gachon University, Yeonsu-gu, Incheon 406-799, Republic of Korea

Supporting Information

ABSTRACT: Salinazinones A (1) and B (2), two unprecedented pyrrolidinyl-oxazinones, were isolated from the culture broth of *Streptomyces* sp. KMF-004 from a solar saltern at Aphae Island, Korea. The structures of these salinazinones, which are unusual and consist of 2-methylpropenyl-1,3-oxazin-6-one bearing 1-oxopyrrolidinyl substituents, were assigned by spectral and chemical analyses using Mosher's method, circular dichroism (CD), and calculated ECD. Salinazinones are the first examples of a natural alkaloid class composed of an oxazinone–pyrrolidone conjugate.



Solar salterns, which have not been extensively investigated, are composed of a series of shallow ponds in which seawater is gradually concentrated to precipitate sodium chloride and other valuable minerals via solar heat and wind. Recently, various halophilic archaea and bacteria have been identified in the hypersaline environment of solar salterns via culture- or nonculture-based studies.¹

As part of our ongoing program to explore new secondary metabolites from marine actinomycetes, we isolated a bacterial strain, *Streptomyces* sp. KMF-004, from a solar saltern at Aphae Island in Korea. Based on LC-MS analysis using our in-house UV database along with the MarinLit database, two components were identified in the culture broth of the KMF-004 strain and found to possess an unusual chromophore that has not been assigned to any other known metabolites.² A subsequent large-scale cultivation (16 L) in liquid medium led to the isolation of two unknown metabolites using diverse chromatographic methods. The structures of these compounds consist of an unprecedented oxazinone–pyrrolidone conjugate.

Oxazine structures have attracted substantial synthetic interest because of their valuable synthetic intermediates and their biological activities, such as sedative, analgesic, antipyretic, antitumor, and antimicrobial effects.³ 1,3-Oxazin-6-ones are six-membered heterocyclic compounds that are important substrates in heterocyclic transformations.⁴ However, 1,3-oxazin-6-ones have not been thoroughly studied, and most reports on this structure have focused on chemical synthetic studies.³ Some 4-hydroxy-6H-1,3-oxazin-6-ones

exhibit sedative activities and cytotoxicities, which are strongly dependent on the nature of the substituents in the 2- and 5-positions.⁵

Pyrrole is also an important structural building block for numerous natural compounds and well-established drugs, such as Tolmetin, Atorvastatin, Premazepam, Roseophilin, and Zomepirac.^{6,7} Natural compounds containing a pyrrole moiety are present in numerous alkaloids of varying complexity, which have been isolated from diverse natural resources, such as marine organisms, insects, bacteria, fungi, plants, and even vertebrates.⁷ However, the conjugated structure of 6H-1,3-oxazin-6-one and pyrrolidin-2-one has never been reported. Herein, we describe the structural elucidations of two new molecules (1 and 2) based on spectroscopic analyses and chemical methods.

Salinazinone A (1)⁸ was isolated as a yellowish gum. Its molecular formula was determined to be C₁₃H₁₆N₂O₄ based on a pseudomolecular ion at *m/z* 265.1187 [M + H]⁺ using HRFABMS data coupled with ¹³C NMR data. The ¹H NMR spectrum of 1 exhibited four methine proton signals (δ_{H} 6.78, 5.94, 4.65, and 4.49), a methylene group (δ_{H} 2.69 and 2.61), three methyl doublets (δ_{H} 2.28, 2.03, and 1.28), and a doublet signal of an exchangeable proton (δ_{H} 3.42) (Table 1).

The ¹³C NMR spectrum exhibited 13 carbon signals, including two carbonyl carbon signals (δ_{C} 174.2 and 161.5) and three quaternary carbon signals that appeared downfield

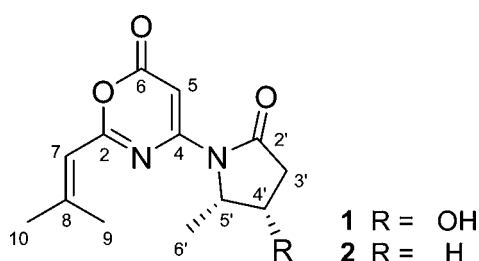
Received: August 31, 2015

Published: October 8, 2015

Table 1. NMR Spectroscopic Data for **1** and **2** in Acetonitrile- d_3

no.	1			2		
	δ_C^a		δ_H mult (J, Hz) ^b	δ_C^a		δ_H mult (J, Hz) ^b
2	165.2	C		165.1	C	
4	156.8	C		157.0	C	
5	90.8	CH	6.78 s	90.0	CH	6.84 s
6	161.5	C		161.6	C	
7	117.4	CH	5.94 br m	117.4	CH	5.94 br m
8	159.6	C		159.4	C	
9	21.5	CH ₃	2.28 d (1.3)	21.5	CH ₃	2.28 d (1.3)
10	28.5	CH ₃	2.03 d (1.3)	28.5	CH ₃	2.03 d (1.3)
2'	174.2	C		177.0	C	
3'	40.5	CH ₂	α : 2.69 dd (17.0, 7.8) β : 2.61 dd (17.0, 9.3)	32.4	CH ₂	α : 2.76 ddd (17.6, 11.3, 9.1) β : 2.44 ddd (17.6, 9.4, 2.1)
4'	65.8	CH	4.49 dddd (9.3, 7.8, 6.5, 4.8)	25.8	CH ₂	α : 2.25 m/ β : 1.75 m
5'	58.9	CH	4.65 dq (6.5, 6.5)	55.5	CH	4.72 dqd (8.0, 6.4, 1.6)
6'	13.7	CH ₃	1.28 d (6.5)	20.5	CH ₃	1.33 d (6.4)
4'-OH			3.42 d (4.8)			

^a¹³C NMR experiment was performed at 100 MHz. ^b¹H NMR and gHSQC experiments were performed at 400 MHz.



from 150 ppm (δ_C 165.2, 159.6, and 156.8) (Table 1). The interpretation of the 2D NMR spectral data allowed for the construction of two structural fragments (Figure 1).

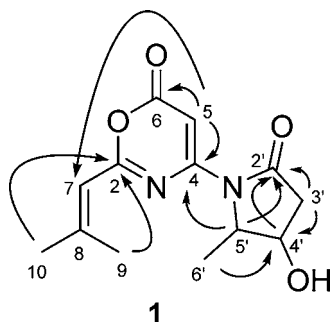


Figure 1. Key HMBC correlations in **1**.

One fragment, 2-methylpropenyl-1,3-oxazin-6-one, was established by interpreting the HMBC correlations from H-5 (δ_H 6.78) to C-4 (δ_C 156.8), C-6 (δ_C 161.5), and C-7 (δ_C 117.4). The HMBC correlation across five bonds from H-5 to C-7 provided valuable information for the 1,3-oxazin-6-one moiety. Standard HMBC spectra usually show correlations across either two or three bonds. However, five bond long-range couplings can sometimes be found in quinones and heteroaromatic-like compounds.⁹ The observation of ⁵J_{C,H} correlations in these structural classes depends on the pattern and nature of the substituents, and 1,3-oxazin-6-one bearing a vinyl substituent could be a good example of ⁵J_{C,H} coupling in a standard gHMBC experiment. The presence of the 2-methylpropenyl group was supported by the HMBC correlations from H-7 (δ_H 5.94) to C-9 (δ_C 21.5) and C-10

(δ_C 28.5). The HMBC correlations from H₃-9 and H₃-10 to C-2 (δ_C 165.2) permitted the 2-methylpropenyl group to be positioned at C-2 of the oxazinone ring. In addition, the strong NOE correlation between H-7 and H₃-10 (δ_H 2.03) was observed in the NOESY spectrum of **2**, whereas there was no NOE correlation between H-7 and H₃-9 (δ_H 2.28). This NOE correlation allowed us to assign the geometric relationship of H-7 and H₃-10 as a *cis* configuration (Figure S2). The ¹H–¹H COSY correlations corresponding to the connectivity from C-3' to C-6' as well as the HMBC correlation of H-5' (δ_H 4.65) and C-2' (δ_C 174.2) allowed for the construction of the other fragment, 4-hydroxy-5-methylpyrrolidin-2-one. The connection between the two fragments was identified based on the HMBC correlations from H-5' to C-4.

The relative configuration at C-4' and C-5' of **1** can be assigned as a *syn* orientation for H-4' and H-5' based on the NOE correlation between 4'-OH and H₃-6, as well as the NOE correlation between H-4' and H-5' (Figure S2). The absolute configurations for C-4' and C-5' of **1** were determined by applying the modified Mosher's method.¹⁰ Separate treatment of **1** in pyridine with (R)-(-)- α -methoxy- α -(trifluoromethyl) phenylacetyl chloride [(R)-MTPA-Cl] and (S)-MTPA-Cl yielded the (S)-(**1-Ma**) and (R)-Mosher esters (**1-Mb**), respectively. Analysis of the ¹H chemical shift differences ($\Delta\delta_{S,R}$) between **1-Ma** and **1-Mb** revealed negative values for H₂-3' but positive values for H-5' and H₃-6' (Figure S3). These data allowed the absolute configurations of C-4' and C-5' of **1** to be assigned as *S* and *S*, respectively. Therefore, the structure of salinazinone A (**1**) was determined to be 4-((4*S*,5*S*)-4-hydroxy-5-methyl-2-oxopyrrolidin-1-yl)-2-(2-methylprop-1-en-1-yl)-6*H*-1,3-oxazin-6-one.

Salinazinone B (**2**)¹¹ was obtained as a pale yellowish gum with a molecular formula of C₁₃H₁₆N₂O₃ based on HRFABMS data (obsd [M + H]⁺ at *m/z* 249.1241). The molecular formula indicated that **2** possessed one fewer oxygen atom than **1**. The UV and IR spectra of **2** were nearly identical to those of **1**, suggesting a structural scaffold similar to that of **1**. As was done for salinazinone A (**1**), a comprehensive analysis of the 2D NMR data of **2** allowed for the complete assignment of the proton and carbon signals, leading to the construction of a planar structure for **2**. Unlike

1, the ^1H spectral data of **2** indicated no exchangeable hydroxyl protons and aliphatic methylene protons (δ_{H} 2.25 and 1.75) rather than the H-4' methine proton of **1** (Table 1). Therefore, the structure of salinazinone B (**2**) was determined to be a dehydroxylated analogue of **1**.

The absolute configuration of C-5' in **2** was assigned by comparing its circular dichroism (CD) spectrum with the calculation of the electronic circular dichroism (ECD) spectra, coupled with analysis of NOE correlations in the NOESY experiment. Because two heterocyclic chromophores, an oxazinone and a pyrrolidinone, are connected by the N–C bond (N atom exist as bridge tail) and no NOE correlations between H-5 and any protons of the pyrrolidinone moiety are observed in **2**, there could be four supposable stereochemical structures depending on the rotation directions of two chromophores¹² and the absolute configuration at C-5' (Figure S4). The measured CD spectrum of **2** was similar to that of **1**, and both spectra exhibited a distinct negative Cotton effect at 250 nm, which are consistent with the calculated ECD spectra of **1a** and **2a** (Figure 2). The NOESY

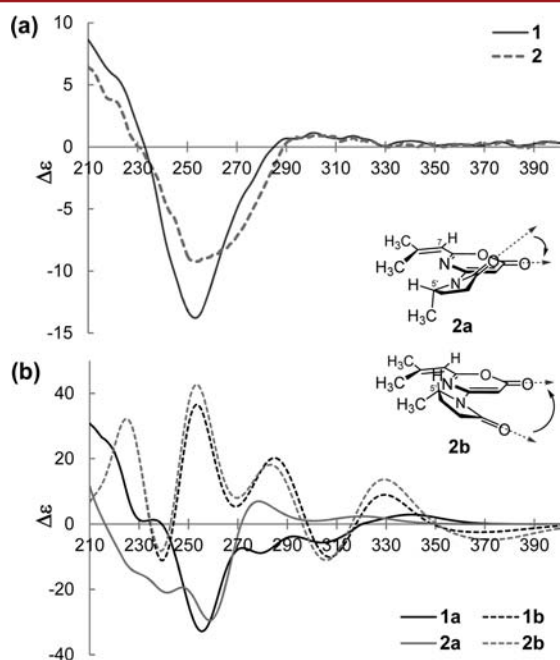


Figure 2. (a) CD data for **1** and **2**. (b) Calculation of ECD data for **1a**, **1b**, **2a**, and **2b**.

spectrum of **2** showed the correlation between H-5' and H₃-9, while no NOE correlation between H₃-6' and H₃-9 was observed (Figure 3). Thus, the possible direction of two heterocyclic chromophores and the NOE correlation (H-5' and H₃-9) allowed us to assign the absolute configurations at C-5' of **2** as *S* (Figure 3).

The core structures of salinazinones A and B are unprecedented in the alkaloid literature.¹³ In addition, to the best of our knowledge, the 6*H*-1,3-oxazin-6-one core of **1** and **2** has not been previously observed in natural products.

Although further exploration of the related intermediates is needed to gain insight into their biogenetic pathway, we discovered a new demethylated bohemamine derivative, which is referred to as bohemamine D (**3**) (Scheme 1), along with bohemamine B which was reported from a marine-derived *Streptomyces* sp.¹⁴ Bohemamine D (**3**)¹⁵ was isolated as a pale

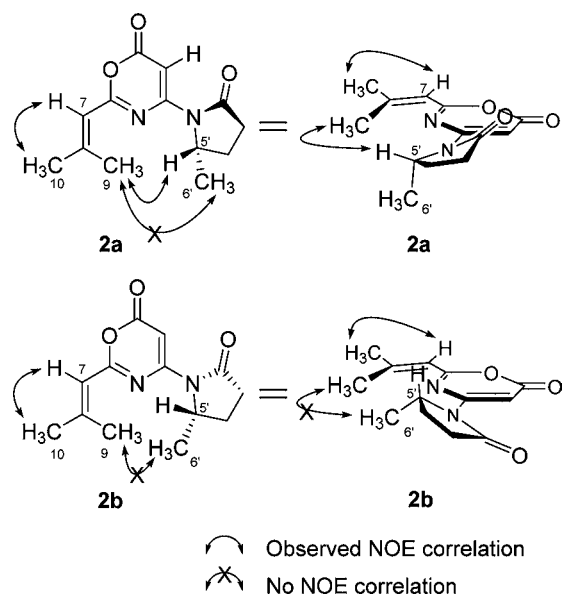
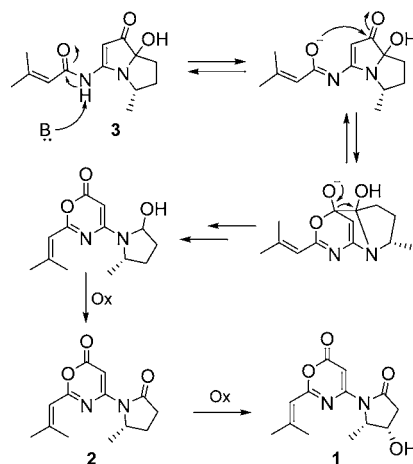


Figure 3. Two supposable conformations of **2** (**2a** and **2b**).

Scheme 1. Plausible Biosynthetic Pathway for **1** and **2** from Bohemamine D (**3**)



yellowish gum. The molecular formula was determined to be $\text{C}_{13}\text{H}_{18}\text{N}_2\text{O}_3$ based on HRFABMS data ($[\text{M} + \text{H}]^+$ at m/z 251.1391). The UV spectrum was nearly identical to those reported for other bohemamines.¹⁴ The 1D and 2D NMR spectral data for **3** were similar to those of NP25302, which was isolated from *Streptomyces* sp. UMA-044.¹⁶ Comprehensive analysis of the 2D NMR data for **3** allowed the complete assignment of the proton and carbon signals, leading to the construction of a planar structure for **3**. Unlike the known compound NP25302, the ^1H NMR and HMBC spectral data of **3** indicated the presence of a hydroxyl group at the C-7 position of **3** instead of the methyl group in NP25302. The absolute configurations of the chiral centers have not been determined. The demethylated bohemamine at the C-7 position may be the result of another biosynthetic pathway in previously reported bohemamine series, and **3** is a possible key precursor for the biosynthesis of **1** and **2**.

A plausible biosynthetic pathway for **1** and **2** is proposed in Scheme 1. The key intermediate (**3**) is expected to be synthesized in a manner similar to that proposed by Fu and MacMilan.¹⁷ The amide in **3** serves as a nucleophile for the

cyclization that forms the oxazinone scaffold. Prior to the production of oxazinone, cleavage of the carbon–carbon bond results in the formation of the pyrrolidine ring system, and further oxidation generates **2** and **1**. This type of cyclization process, which is accompanied by C–C bond cleavage to form oxazinone, is unusual, and the typical mechanism involves leaving a general electron-withdrawing atom or group.¹⁸ In this context, it would be interesting to identify the enzyme involved in this cyclization reaction. The genome of *Streptomyces* sp. TP-A0873, a bohemamine-producing bacterium, was recently sequenced, but the biosynthetic gene cluster has not yet been revealed.¹⁹ Therefore, the elucidation of the biosynthesis of salinazinones and bohemamines will be the aim of our next study, in which the genomic sequences of the two producers, *Streptomyces* sp. KMF-004 and TP-A0873, will be investigated.

Compounds **1–4** were tested for their biological activities against LPS-induced NO production by BV-2 microglia cells. Salinazinone B (**2**) inhibited the NO production with IC₅₀ values of 17.7 μM (positive control L-NMMA IC₅₀ 19.6 μM) without any cellular toxicity in BV-2 microglia cells compared to the LPS treated group, whereas salinazinone A (**1**) was found to be inactive (IC₅₀ 162 μM) (Table S3).

■ ASSOCIATED CONTENT

■ Supporting Information

The Supporting Information is available free of charge on the ACS Publications website at DOI: 10.1021/acs.orglett.5b02495.

General experimental procedures, bioassay protocols, and spectroscopic data of **1–4** (PDF)

Crystallographic data of **4** (CIF)

■ AUTHOR INFORMATION

Corresponding Author

*E-mail: hkwon@kist.re.kr.

Author Contributions

#M.C.K. and J.H.L. contributed equally.

Notes

The authors declare no competing financial interest.

■ ACKNOWLEDGMENTS

The present study was supported by the Korea Institute of Science and Technology institutional program (2Z04371) and by the Korea Institute of Oriental Medicine, under Grant Number K15310.

■ REFERENCES

- (1) (a) Oren, A. *FEMS Microbiol. Ecol.* **2002**, *39*, 1. (b) Ghai, R.; Pašić, L.; Fernández, A. B.; Martín-Cuadrado, A.-B.; Mizuno, C. M.; McMahon, K. D.; Papke, R. T.; Stepanauskas, R.; Rodríguez-Brito, B.; Rohwer, F.; Sánchez-Porro, C.; Ventosa, A.; Rodríguez-Valera, F. *Sci. Rep.* **2011**, *1*, 135.
- (2) (a) Laatsch, H. *AntiBase 2005, The Natural Compound Identifier*; Wiley-VCH: Weinheim, Germany, 2005. (b) Blunt, J. W. *MarinLit 2012, A Database of the Marine Natural Products Literature*; Royal Society of Chemistry: London, 2015.
- (3) Sindhu, T. J.; Arikkatt, S. D.; Vincent, G.; Chandran, M.; Bhat, A. R.; Krishnakumar, K. *Int. J. Pharm. Sci. Res.* **2013**, *4*, 134.
- (4) Steglich, W.; Jeschke, R.; Buschmann, E. *Gazz. Chim. Ital.* **1986**, *116*, 361.

(5) Lalaev, B. Y.; Petina, O. A.; Kuz'mich, N. N.; Yakovlev, I. P.; Alekseeva, G. M.; Zakhs, V. E. *Russ. J. Gen. Chem.* **2006**, *76*, 645.

(6) Sharma, R.; Chouhan, M.; Nair, V. A. *Tetrahedron Lett.* **2010**, *51*, 2039.

(7) Domagala, A.; Jarosz, T.; Lapkowski, M. *Eur. J. Med. Chem.* **2015**, *100*, 176.

(8) Salinazinone A (**1**): yellowish gum; $[\alpha]_D^{20}$ +3.6 (c 0.06, CH₃OH); CD (CH₃OH) λ_{max} ($\Delta\epsilon$) 205 (+9.33), 250 (−13.14) nm; UV (CH₃CN) λ_{max} (log ϵ) 244 (4.30), 314 (3.63) nm; IR (film) ν_{max} 3435, 2988, 2936, 1742, 1644, 1593, 1541, 1393, 1356, 1272, 1101, 1070 cm^{−1}; ¹H and ¹³C NMR spectra, see Table 1; HRFABMS [M+H]⁺ *m/z* 265.1187 (calcd for C₁₃H₁₇N₂O₄, 265.1188).

(9) (a) Araya-Maturana, R.; Pessoa-Mahana, H.; Weiss-López, B. *Nat. Prod. Commun.* **2008**, *36*, 271. (b) Tapia, R. A.; Prieto, Y.; Pautet, F.; Fenet, B.; Fillion, H. *Magn. Reson. Chem.* **2002**, *40*, 165.

(10) Séco, J. M.; Quiñoa, E.; Riguera, R. *Tetrahedron: Asymmetry* **2001**, *12*, 2915.

(11) Salinazinone B (**2**): pale yellowish gum; $[\alpha]_D^{20}$ +1.6 (c 0.13, CH₃OH); CD (CH₃OH) λ_{max} ($\Delta\epsilon$) 205 (+6.77), 250 (−6.77) nm; UV (CH₃CN) λ_{max} (log ϵ) 254 (4.30), 318 (3.73) nm; IR (film) ν_{max} 2926, 2854, 1725, 1632, 1548, 1536, 1440, 1378, 1291, 1131, 1076 cm^{−1}; ¹H and ¹³C NMR spectra, see Table 1; HRFABMS [M+H]⁺ *m/z* 249.1241 (calcd for C₁₃H₁₇N₂O₃, 249.1239).

(12) Bringmann, G.; Tasler, S.; Endress, H.; Kraus, J.; Messer, K.; Wohlfarth, M.; Lobin, W. *J. Am. Chem. Soc.* **2001**, *123*, 2703.

(13) *The Alkaloids: Chemistry and Biology*; Knölker, H.-J., Ed.; Academic Press: Waltham, MA, 2015; Vol. 74, pp 1–410, and earlier volumes in this series.

(14) Bugni, T. S.; Woolery, M.; Kauffman, C. A.; Jensen, P. R.; Fenical, W. *J. Nat. Prod.* **2006**, *69*, 1626.

(15) Bohemamine D (**3**): pale yellowish gum; $[\alpha]_D^{20}$ −0.7 (c 0.09, CH₃OH); UV (CH₃CN) λ_{max} (log ϵ) 248 (4.30), 292 (3.89), 335 (3.87) nm; IR (film) ν_{max} 3218, 2976, 2933, 1713, 1650, 1563, 1504, 1447, 1380, 1204, 1133, 1058 cm^{−1}; ¹H and ¹³C NMR spectra, see Table S2; HRFABMS [M+H]⁺ *m/z* 251.1391 (calcd for C₁₃H₁₉N₂O₃, 251.1396).

(16) Zhang, Q.; Schrader, K. K.; ElSohly, H. N.; Takamatsu, S. *J. Antibiot.* **2003**, *56*, 673.

(17) Fu, P.; MacMillan, J. B. *Org. Lett.* **2015**, *17*, 3046.

(18) (a) Riva, R.; Banfi, L.; Basso, A.; Zito, P. *Org. Biomol. Chem.* **2011**, *9*, 2107. (b) Slowinski, F.; Ayad, O. B.; Ziyaret, O.; Botuha, C.; Le Falher, L. L.; Aouane, K.; Thorimbert, S. *Org. Lett.* **2013**, *15*, 3494. (c) Molina, P.; Conesa, C.; Velasco, M. D. *Tetrahedron Lett.* **1993**, *34*, 175.

(19) Komaki, H.; Ichikawa, N.; Hosoyama, A.; Fujita, N.; Igarashi, Y. *Genome Announce* **2015**, *3*, e00008-15.